MicroRNA-199a-3p suppresses high glucose-induced apoptosis and inflammation by regulating the IKKβ/NF-κB signaling pathway in renal tubular epithelial cells

RUIMIN ZHANG, LINFANG QIN and JUN SHI

Department of Nephrology, Huaihe Hospital of Henan University, Kaifeng, Henan 475000, P.R. China

Abstract. Renal tubular epithelial cells (RTEC) injury induced by hyperglycemia is considered a major contributor to the pathogenesis of diabetic nephropathy (DN). However, few studies have focused on the role of microRNAs (miRNAs/miRs) in RTEC injury. Therefore, the present study aimed to investigate the role and mechanisms of miRNAs in RTEC injury. In the study, miRNAs expression profiles were determined via microarray assay in the peripheral blood samples of patients with DN. High glucose (HG)-induced injury in HK-2 cells was used as a cell model to examine the potential role of miR-199a-3p in DN. The expression of miR-199a-3p was validated using reverse transcription-quantitative PCR. The expressions of TNF-α, IL-1β and IL-6, were detected via ELISA. The protein levels of apoptosis-related proteins were determined using western blotting. Cell apoptosis and caspase 3 activity were evaluated via flow cytometry analysis and caspase 3 activity assay, respectively. Luciferase reporter assay was used to confirm the interaction between miR-199a-3p and IKKβ. miR-199a-3p was found to be significantly downregulated in the peripheral blood samples, and there was a negative correlation between miR-199a-3p expression and proteinuria in patients with DN. It was identified that miR-199a-3p expression was time-dependently decreased in the HG-induced cell damage model. Moreover, miR-199a-3p overexpression significantly improved HG-induced cell injury, as evidenced by the decrease in cell apoptosis and inflammation. Subsequent analyses demonstrated that miR-199a-3p directly targeted IKKβ, whose expression was increased, and negatively correlated with miR-199a-3p expression in patients with DN. The protective effects of miR-199a-3p overexpression on HG-treated HK-2 cells were partially reversed by IKKβ overexpression. In addition, activation of the NF-κB pathway by HG was blocked by miR-199a-3p mimics transfection in HK-2 cells. Collectively, the present findings indicated that miR-199a-3p protected HK-2 cells against HG-induced injury via inactivation of the IKKβ/NF-κB pathway, suggesting enhanced expression of miR-199a-3p as a potential therapeutic strategy for patients with DN.

Introduction

Diabetic nephropathy (DN) is a common complication of diabetes mellitus, and 30-40% of all diabetic patients will ultimately develop DN (1). The destructive role of renal tubular epithelial cell (RTEC) apoptosis in DN progression has been reported by clinical and basic research (2,3). Therefore, inhibition of RTEC damage may be an effective treatment strategy to block the occurrence and development of DN.

MicroRNAs (miRNAs/miRs) are a class of single-stranded, small non-coding RNAs (21-25 nucleotides), which degrade or inhibit their target genes at the post-transcriptional level (4). Numerous studies have reported the involvement of miRNAs in the progression of diabetes complications, especially DN (5-7). For instance, miR-93 can prevent the progression of DN by downregulating the promoter of the host minichromosome maintenance complex component 7 gene (8). Wang *et al* (9) observed that miR-21 contributed to renal fibrosis by targeting MMP-9 in a mouse model of DN. Furthermore, several studies have revealed that miRNAs are involved in high glucose (HG)-mediated apoptosis in RTEC. For example, Li *et al* (10) found that miR-25 was associated with RTEC apoptosis via the PTEN/AKT pathway. Moreover, overexpression of miR-23c inhibits the apoptosis of RTEC by targeting ELAV like RNA binding protein 1 (11). Since the central role of RTEC injury in DN has been extensively studied (12), identifying additional miRNAs that are involved in the regulation of the RTEC injury could provide further in-depth understanding of the pathogenesis of DN.

In the present study, the miRNA expression profile was examined in peripheral blood from patients with DN using a microarray assay, and the most downregulated of these, miR-199a-3p, was selected for further analysis. Using a HG-induced RTEC injury model, the functional role of miR-199a-3p in RTEC injury and the underlying mechanisms were investigated.

Correspondence to: Dr Jun Shi, Department of Nephrology, Huaihe Hospital of Henan University, 115 Ximen Avenue, Gulou, Kaifeng, Henan 475000, P.R. China
E-mail: junshijsjl@163.com

Materials and methods

Tissue samples. Peripheral blood samples (10 ml) were collected from 30 patients with DN and 30 healthy controls at the Department of Nephrology, Huaihe Hospital of Henan University between May 2017 and June 2018. The patients with DN included 13 men and 17 women with a mean age of 34.2 years (age range, 21-62 years), while the healthy controls included 11 men and 19 women with a mean age of 32.1 years (age range, 20-60 years). The study was approved by the Research Ethics Committee of Huaihe Hospital of Henan University. Written informed consent was obtained from all patients.

Cell culture and treatment. HK-2 cells were obtained from the American Type Culture Collection, and were cultured in DMEM (Thermo Fisher Scientific, Inc.) with 8% FBS (Gibco; Thermo Fisher Scientific, Inc.) and 1% penicillin-streptomycin (Beyotime Institute of Biotechnology) in a 5% CO_2 incubator at 37°C. When HK-2 cells reached 90% confluence, the serum was withdrawn for 24 h and the media were changed to serum-free DMEM containing 5.5 mmol/l glucose or 30 mM glucose (Sigma-Aldrich; Merck KGaA) (13-15). At 6, 12, 18 and 24 h after treatment, the expression of miR-199a-3p in HK-2 cells was analyzed using reverse transcription-quantitative (RT-q)PCR.

miRNA microarray. The microRNA array was performed by Kangcheng Bio-Tech, Inc. Total RNA was isolated from peripheral blood of patients with DN and controls using a miRNeasy kit (Qiagen, Inc.). The RNA purity was determined via NanoDrop ND-1000 spectrophotometry (Thermo Fisher Scientific, Inc.) and the RNA quality was determined using 1% agarose-formaldehyde denaturing gel electrophoresis. After RNA quantitation, the samples were assessed using the miRCURY LNA™ Array v. 16.0 (Exiqon A/S; Qiagen, Inc.) according to the manufacturer's protocol. The procedure and imaging processes were performed as described previously (16). The microarray data were analyzed using Agilent Feature Extraction software (version 10.7; Agilent Technologies, Inc.) (17). Differentially expressed miRNAs were screened with an unpaired t-test (P<0.05) combined with a significant threshold value of a fold change [FC; (log2 (FC) >2 for upregulated, and log2 (FC) ≤-2 for downregulated]. The microarray data that support the findings of this study are available from the corresponding author upon reasonable request.

RT-qPCR. Total RNA was extracted from peripheral blood samples or cells using TRIzol® reagent (Thermo Fisher Scientific, Inc.). cDNA was synthesized using PrimeScript One Step RT-PCR kit (Takara Biotechnology Co., Ltd.) for 60 min at 42°C. RT-qPCR was performed using the SYBR Green PCR kit (Toyobo Life Science) on an ABI 7500 system (Thermo Fisher Scientific, Inc.). The primers for RT-qPCR analysis were as follows: miR-199a-3p forward, 5'-TACAGGACCGGTCGACTAGG-3' and reverse, 5'-CTCGCTTCGGCAGCACA-3'; U6 forward, 5'-TGCGGG TGCTCGCTTCGCAGC-3' and reverse, 5'-CCAGTGCAG GGTCCGAGGT-3'; IKKβ forward, 5'-AGCTCTGGAACC TCCTGAAGA-3' and reverse, 5'-AGCTCCAGTCTAGGG

TCGTGA-3'; and GAPDH forward, 5'-AGGTCGGTGTGA ACGGATTTG-3' and reverse: 5'-TGTAGACCATGTAGTTGA GGTCA-3'. The reaction mixtures were denatured at 95°C for 3 min, followed by 40 two-step cycles of 95°C for 10 sec and 60°C for 30 sec. Relative quantification was determined via normalization to U6 or GAPDH. The relative expression levels were calculated based on the $2^{-\Delta\Delta Cq}$ method (18).

Cell transfection. HK-2 cells ($5x10^5$/well) were seeded in a 6-well plate overnight, and then cells were transfected with 20 nM miR-199a-3p mimics, 20 nM mimics negative control (NC), 20 nM miR-199a-3p inhibitor, 20 nM inhibitor NC, 2 µg pcDNA-IKKβ or pcDNA3.1-vector (Shanghai GenePharma Co., Ltd.) using Lipofectamine® 2000 (Invitrogen; Thermo Fisher Scientific, Inc.). The sequences were as follows: miR-199a-3p mimics, 5'-ACAGUAGUCUGCACAUUGGUU A-3'; mimics NC, 5'-GGACCAAATCTCGAGATTTGG-3'; miR-199a-3p inhibitor, 5'-UAACCAAUGUGCAGACUACUG U-3'; and inhibitor NC, 5'-TTCTCCGAACGTGTCACGTTT C-3'. After 24 h transfection, HK-2 cells were stimulated with HG (30 mM) for 24 h at 37°C, and then protein and RNA were extracted for analyses.

Cell Counting Kit-8 (CCK-8) assay. After 24 h transfection, HK-2 cells ($5x10^3$) were stimulated with HG (30 mM) for 24 h at 37°C, and then cell viability in 96-well plates was evaluated using CCK-8 assay according to the manufacturer's instructions. Briefly, 10 µl CCK-8 solution (Dojindo Molecular Technologies, Inc.) was added to each well and incubated at 37°C for another 2 h. The absorbance at 450 nm was measured using a microplate reader (Bio-Rad Laboratories, Inc.).

Flow cytometry assay. After 24 h transfection, HK-2 cells were stimulated with HG (30 mM) at 37°C for 24 h, and then apoptosis was evaluated using Annexin V/PI apoptosis-detection kit (Nanjing KeyGen Biotech Co., Ltd.), according to the manufacturer's protocols. The cells were harvested by ice-cold PBS and stained with FITC-Annexin V and PI in binding buffer for 15 min at room temperature in the dark. Then, cell apoptosis were detected with an EPICS XL-MCL FACScan flow cytometer (Becton, Dickinson and Company) and analyzed using FlowJo 8.7.1 software (FlowJo LLC). The results indicated healthy viable cells in the lower left quadrant (Q4) on the scatter plot as (FITC-/PI-). The lower right quadrant (Q3) represented the early stage apoptotic cells as (FITC+/PI-). The upper right quadrant (Q2) represented necrotic cells and late stage apoptotic cells as (FITC+/PI+). Apoptotic rate = percentage of early stage apoptotic cells (Q3) + percentage of late stage apoptotic cells (Q2). The experiment was repeated three times independently.

Caspase-3 activity assay. After 24 h transfection, HK-2 cells were stimulated with HG (30 mM) at 37°C for 24 h, and cells ($5x10^3$/well) were collected and lysed using RIPA lysis buffer (Beyotime Institute of Biotechnology). Then, caspase-3 activity in was determined using a caspase-3 Activity Assay kit (Beyotime Institute of Biotechnology), according to the manufacturer's protocol. The optical density was measured at a wavelength of 450±2 nm using a microplate reader (Bio-Rad Laboratories, Inc.).

ELISA assay. After 24 h transfection, HK-2 cells were stimulated with HG (30 mM) at 37˚C for 24 h, and then the levels of IL-6 (cat. no. p1330), IL-8 (cat. no. p1640) and TNF-α (cat. no. pt518) were evaluated using commercial ELISA kits (Beyotime Institute of Biotechnology).

Vector construction. Luciferase reporters were generated based on the firefly luciferase expressing vector pGL3-control (Promega Corporation). To construct pGL3-IKKβ-3' untranslated region (UTR), a partial 3'UTR of the IKKβ segment of human IKKβ mRNA containing the putative miR-199a-3p binding sites was amplified and cloned into the vector pGL3-control. Mutations within the potential miR-199a-3p binding sites were introduced using a QuikChange Site-Directed Mutagenesis kit (Thermo Fisher Scientific, Inc.). Following sequencing, the recombinant segment of the correct clone was incised by *Bam*HI and *Xba*I (Takara Bio, Inc.). The recombinant segment was inserted into pGL3 vector, which was incised by the same two restriction endonucleases. The clones were sequenced, and the correct clones were amplified and identified before transfection.

Luciferase assays. TargetScan 7.0 (http://www.targetscan.org) and PicTar (https://pictar.mdc-berlin.de/; release 2007) were used to search for the putative targets of miR-199a-3p. The dual-luciferase reporter assay was performed as described previously (19). HK-2 cells were transfected with 20 nM miR-199a-3p or inhibitor and the luciferase reporter plasmids using Lipofectamine® 2000 (Invitrogen; Thermo Fisher Scientific, Inc.). After 48 h, luciferase activity was assessed using the dual luciferase reporter kit (Beyotime Institute of Biotechnology). *Renilla* activity was used to normalize firefly luciferase activity.

Western blot analysis. After 24 h transfection, HK-2 cells were stimulated with HG (30 mM) at 37˚C for 24 h. Then, total protein was obtained using RIPA lysis buffer (Beyotime Institute of Biotechnology) and quantified with a BCA protein assay kit (Pierce; Thermo Fisher Scientific, Inc.). Next, the proteins (40 μg/lane) in the lysates were separated via 12% SDS-PAGE and transferred to PVDF membranes (Cytiva). After being blocked with a 5% skim milk solution for 1 h at room temperature, the specific primary antibodies were incubated in the membranes at 4˚C overnight, including IKKβ (cat. no. 8943; 1:1,000), IL-6 (cat. no. 12912; 1:1,000), TNF-α (cat. no. 11948; 1:1,000), Bax (cat. no. 5023; 1:1,000), Bcl-2 (cat. no. 3498; 1:1,000), cleaved-poly(ADP-ribose) polymerase 1 (PARP; cat. no. 5625; 1:1,000), total PARP (cat. no. 9532; 1:2,000), cleaved-caspase-3 (cat. no. 9654; 1:1,000), total caspase-3 (cat. no. 14220; 1:1,000), phosphorylated (p)-IκB-α (cat. no. 2859, 1:1,000), IκB-α (cat. no. 4814; 1:1,000), nuclear p-p65 (cat. no. 3033, 1:1,000), Histone H3 (cat. no. 9728; 1:1,000) and β-actin (cat. no. 4970; 1:2,000). All antibodies were obtained from Cell Signaling Technology, Inc., while IL-8 (cat. no. ab110727; 1:1,000) was obtained from Abcam. Subsequently, the corresponding anti-mouse or anti-rabbit secondary horseradish perxoidase-conjugated antibodies (cat. nos. 7076 and 7074; 1:2,000) were added into the membranes for 2 h at room temperature. The protein bands were visualized using an ECL detection system (Thermo Fisher Scientific, Inc.). Semi-quantification was performed using ImageJ version 1.46 (National Institutes of Health).

Statistical analysis. Statistical analysis was performed using GraphPad Prism (Version 5.0; GraphPad Software, Inc.). Data are presented as the mean ± SD. Differences between groups were analyzed using unpaired Student's t-test or one-way ANOVA followed by Bonferroni post hoc test. Pearson's analyses were used for correlation analysis between miR-199a-3p and IKKβ expression levels. P<0.05 was considered to indicate a statistically significant difference. The experiment was repeated three times independently.

Results

miR-199a-3p is downregulated in peripheral blood of patients with DN. Microarray was used to compare the miRNA patterns between peripheral blood of patients with DN and healthy controls. The miRNA microarray identified 20 miRNAs (e.g miR-146a, miR-214 and miR-503) that were upregulated and 19 miRNAs (e.g miR-199a-3p) that were downregulated by >4-fold in the peripheral blood of patients with DN (Fig. 1A). The volcano plot demonstrates all of the differentially expressed miR between peripheral blood from patients with DN and healthy controls (Fig. 1B). Among these aberrantly expressed miRNAs, miR-146a, miR-214 and miR-503 were increased, which was consistent with previous reports (6,20,21), indicating the reliability of the present microarray. Of the downregulated miRNAs, miR-199a-3p was identified as one of the most significantly downregulated.

Next, RT-qPCR was performed to further detect miR-199a-3p expression in clinical samples (n=30). It was identified that miR-199a-3p expression was significantly downregulated in the DN group, compared with the control group (Fig. 1C). Moreover, a negative correlation was observed between miR-199a-3p and proteinuria in patients with DN (Fig. 1D). Therefore, miR-199a-3p may be a useful biomarker in DN diagnosis and evaluating its severity.

Overexpression of miR-199a-3p suppresses HG-induced the apoptosis in HK-2 cells. As an initial step, an *in vitro* model was established via HG (30 mM) treatment in HK-2 cells, a human RTEC cell line that is widely used for the DN research (22). Then, the expression of miR-199a-3p in HK-2 cells was analyzed at different times (6, 12, 18 and 24 h) using RT-qPCR. Consistent with the results in the clinical samples, HG treatment time-dependently decreased the expression of miR-199a-3p in HK-2 cells (Fig. 2A).

Subsequently, miR-199a-3p mimics and miR-199a-3p inhibitor were transfected into the cultured HK-2 cells, and the effects on cell viability and apoptosis were examined. It was demonstrated that miR-199-3p expression was significantly increased after miR-199a-3p mimics transfection, and decreased after miR-199-3p inhibitor transfection in HK-2 cells (Fig. 2B). According to the results of CCK-8 assay, HG treatment led to a significant decline in the cell viability, compared with the control group; however, the viability was significantly increased after miR-199a-3p mimics transfection (Fig. 2C). Moreover, miR-199a-3p overexpression weakened the HG-induced apoptosis of HK-2 cells (Fig. 2D). It was also
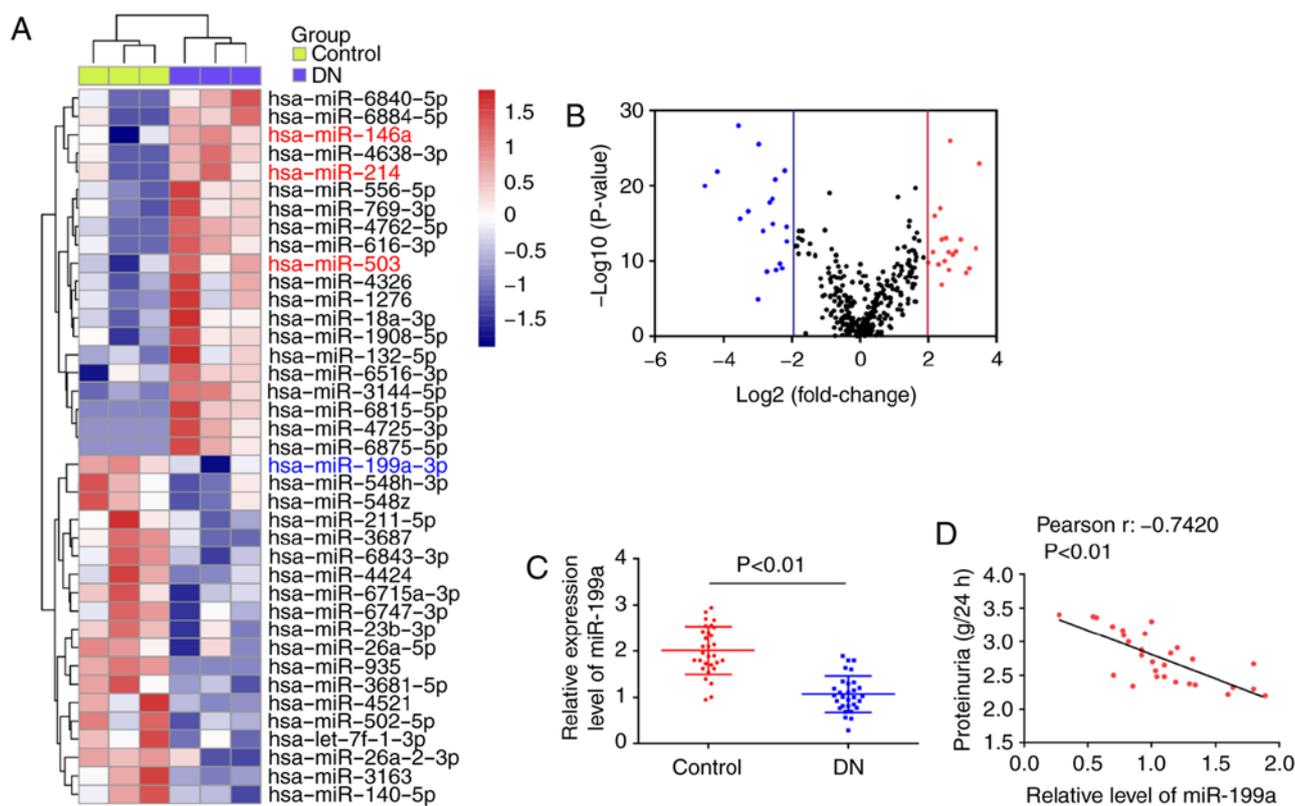
Figure 1. miR-199a-3p is downregulated in peripheral blood from patients with DN. (A) Heatmap of normalized expression levels of miRNAs in peripheral blood from patients with DN and healthy controls (n=3/group). Blue indicates low expression levels, while red indicates high expression levels. (B) Volcano plot presenting the differentially expressed miRs. Y-axis represents log transformed P-value, and x-axis indicates the mean expression differences of miRs between peripheral blood from patients with DN and healthy controls. |log2FoldChange| >2 was set as the cut-off criteria. (C) Expression of miR-199a-3p was determined via reverse transcription-quantitative PCR analysis in 30 peripheral blood samples from patients with DN and 30 peripheral blood samples from healthy controls. (D) Pearson correlation analysis demonstrated a negative correlation between plasma miR-199a-3p expression and proteinuria in 30 patients with DN (r, -0.8752; P<0.01). DN, diabetic nephropathy; miR, microRNA.

found that HG significantly increased the expression levels of Bax, cleaved-caspase-3 and cleaved-PARP, but decreased the expression of Bcl-2 compared with the control group in HK-2 cells; these effects induced by HG were significantly attenuated by miR-199a-3p overexpression (Fig. 2E). Furthermore, miR-199a-3p overexpression weakened the HG-induced caspase-3 activity (Fig. 2F). Collectively, these data suggested that miR-199a-3p could relieve the HK-2 cell apoptosis caused by HG.

Overexpression of miR-199a-3p attenuates the HG-induced inflammatory response in HK-2 cells. It has been reported that the inflammatory response is correlated with DN progression and is an important pathological bases of DN (23). Therefore, the present study examined the influences of miR-199a-3p on the releases of inflammatory cytokines in HG-treated HK-2 cells. The levels of IL-8 (Fig. 3A), IL-6 (Fig. 3B) and TNF-α (Fig. 3C) were significantly increased after HG stimulation, compared with the control group, but overexpression of miR-199a-3p significantly decreased the release of these cytokines in HG-treated HK-2 cells. The protein expression levels of these pro-inflammatory cytokines were also detected via western blotting. Compared with the control group, HG treatment significantly elevated these protein expression levels in HK-2 cells; however, miR-199a-3p overexpression abolished HG-induced effects on protein expression levels

(Fig. 3D). Thus, it was indicated that miR-199a-3p inhibited the HG-induced inflammatory response in HK-2 cells.

miR-199a-3p blocks the activation of the NF-κB pathway in HK-2 cells. In DN, NF-κB is constitutively active and is involved in promoting tubular cell injury, which suggests that inhibiting the activity of NF-κB may constitute a promising therapeutic approach to prevent DN (24,25). Therefore, the influence of miR-199a-3p on the expression levels of key components in the NF-κB pathway were examined in HK-2 cells. HG treatment significantly upregulated the expression levels of IKKβ, p-IκBα and nuclear p-p65, compared with the control group. However, compared with HG group, miR-199a-3p overexpression significantly downregulated these expression levels (Fig. 4A and B). These data demonstrated that miR-199a-3p blocked the activation of the NF-κB signaling pathway, which may be involved in the inhibition of inflammatory mediator release in HG-induced HK-2 cells.

IKKβ is a direct target of miR-199a-3p in HK-2 cells. To evaluate how miR-199a-3p regulates the NF-κB pathway in HG-induced cellular injury *in vitro*, two bioinformatics databases, TargetScan 7.0 (http://www.targetscan.org) and PicTar (https://pictar.mdc-berlin.de/; release 2007), were utilized to predict the targets of miR-199a-3p. IKKβ, one of the upstream molecules of the NF-κB signaling pathway, may
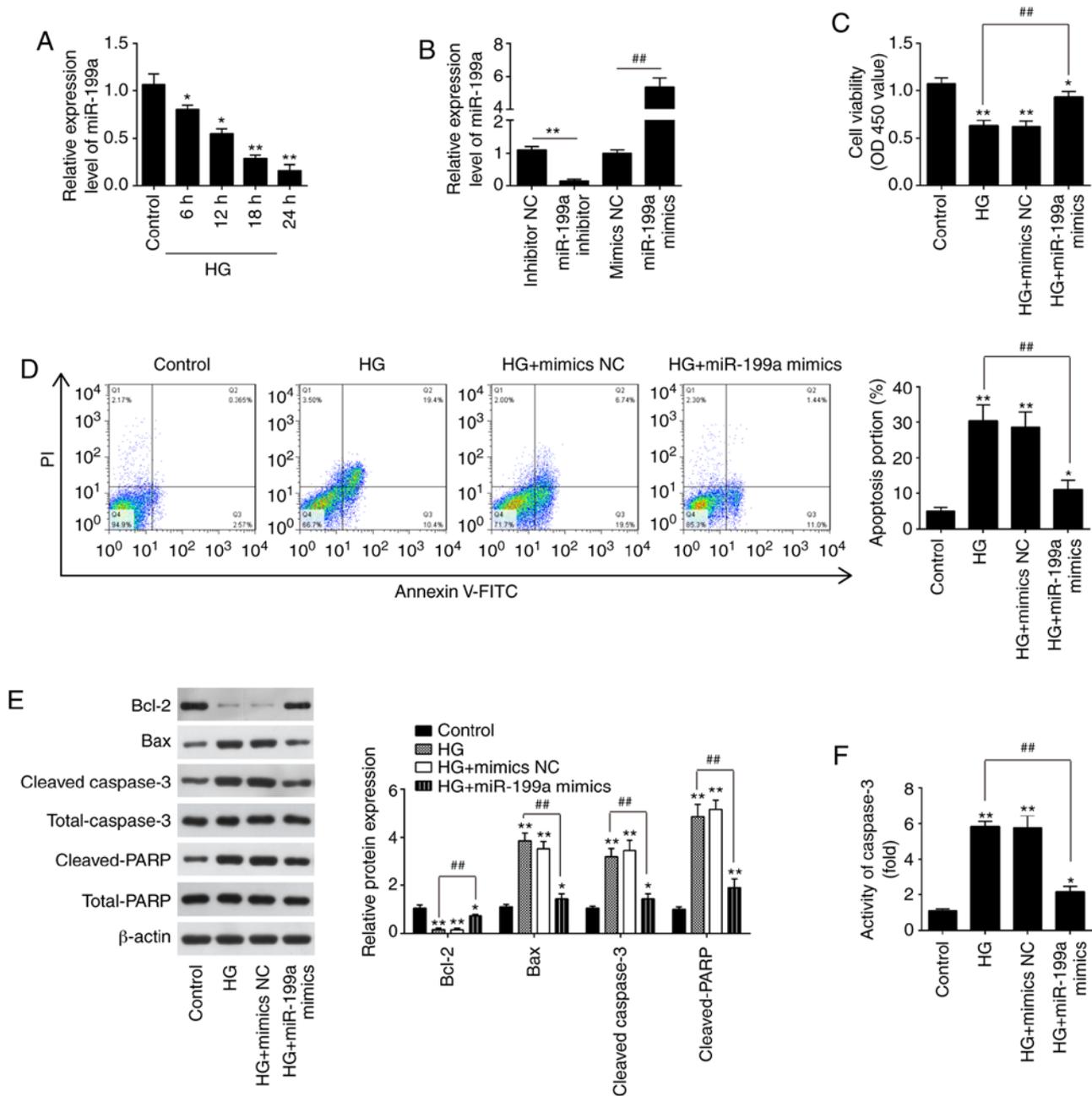
Figure 2. Overexpression of miR-199a-3p inhibits HG-induced HK-2 cell apoptosis. (A) Expression of miR-199a-3p was determined via RT-qPCR analysis at 6, 12, 18 and 24 h after HG treatment. *P<0.05, **P<0.01 vs. Control group. (B) Expression of miR-199a-3p was determined via RT-qPCR analysis 24 h after miR-199a-3p mimics and miR-199a-3p inhibitor transfection. **P<0.01 vs. mimics NC group; ##P<0.01 vs. inhibitor NC group. (C) HK-2 cells were transfected with miR-199a-3p mimics for 24 h, followed by treatment with 30 mM HG for another 24 h, and then cells were harvested for subsequent experiments. Cell viability was assessed using Cell Counting Kit-8 assay. (D) Apoptosis was measured using flow cytometry. (E) Protein expression levels of Bax, Bcl-2, cleaved caspase-3 and cleaved-PARP were measured via western blotting. (F) Activity of caspase-3 was measured using a caspase-3 Activity Assay kit. Data are presented as the mean ± SD of three independent experiments. *P<0.05, **P<0.01 vs. control group; ##P<0.01 vs. HG group. HG, high glucose; miR, microRNA; NC, negative control; PARP, poly(ADP-ribose) polymerase 1; OD, optical density; RT-qPCR, reverse transcription-quantitative PCR.

be a potential target of miR-199a-3p (Fig. 5A). Moreover, it was identified that IKKβ mRNA expression was significantly downregulated by miR-199a-3p mimics transfection, but upregulated by miR-199a-3p inhibitor transfection (Fig. 5B). To experimentally validate whether IKKβ was a direct target of miR-199a-3p, a luciferase reporter assay was performed. The luciferase activity of the IKKβ-3'UTR wild-type was decreased in HK-2 cells after miR-199a-3p mimics transfection, whereas it was increased by miR-199a-3p inhibitor transfection, compared with NC group (Fig. 5C). However, the

luciferase activity of IKKβ-3'UTR mutant reporter plasmid demonstrated no significant change.

The expression of IKKβ was measured in the aforementioned clinical samples, and it was found that IKKβ was significantly upregulated in the DN group compared with the control group (Fig. 5D). Furthermore, a moderate negative correlation between miR-199a-3p and IKKβ expression levels in peripheral blood samples of patients with DN was observed (Fig. 5E). These data indicated that IKKβ was a functional target of miR-199a-3p in HK-2 cells.
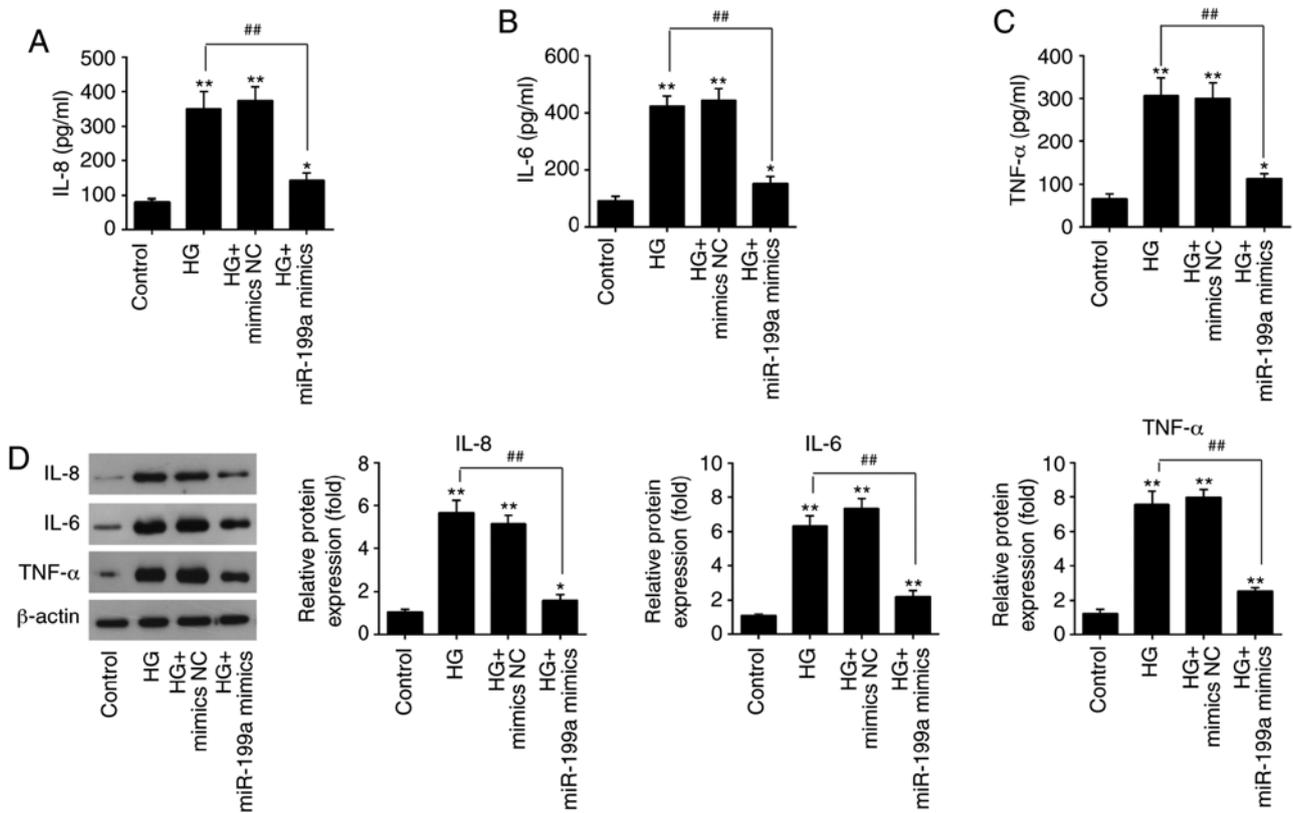
Figure 3. Overexpression of miR-199a-3p attenuates the HG-induced inflammatory response in HK-2 cells. HK-2 cells were transfected with miR-199a-3p mimics for 24 h, followed by treatment with 30 mM HG for another 24 h, and then cells were harvested for subsequent experiments. Levels of (A) IL-8, (B) IL-6 and (C) TNF-α were measured using ELISA kits. (D) Protein expression levels of IL-8, IL-6 and TNF-α were measured via western blotting. Data are presented as the mean ± SD of three independent experiments. *P<0.05, **P<0.01 vs. control group; ##P<0.01 vs. HG group. HG, high glucose; miR, microRNA; NC, negative control.
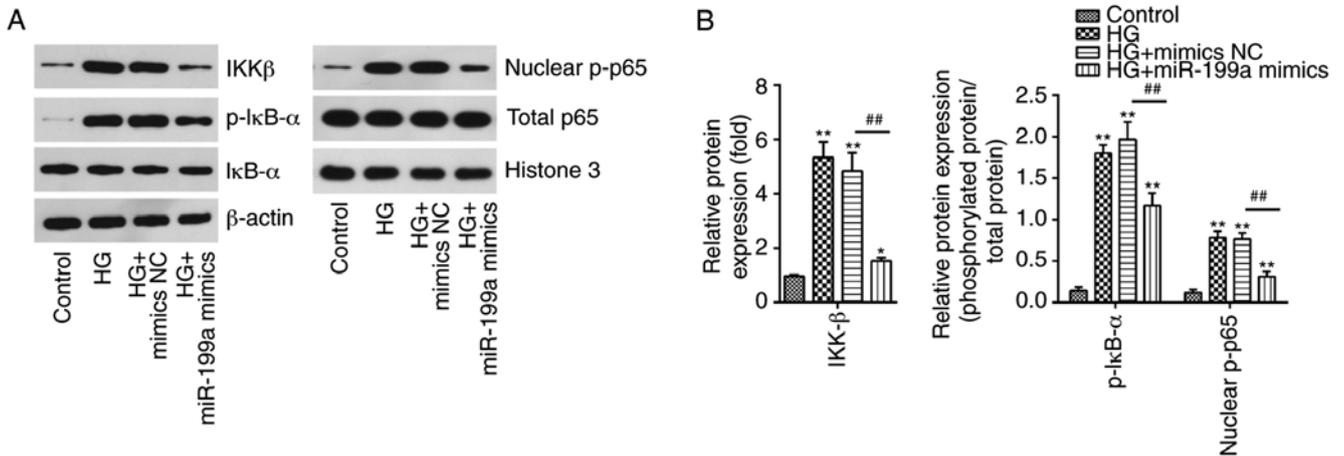

Figure 4. miR-199a-3p blocks the HG-induced activation of the NF-κB pathway. HK-2 cells were transfected with miR-199a-3p mimics for 24 h, followed by treatment with 30 mM HG for another 24 h, and then cells were harvested for subsequent experiments. (A) Protein expression levels of IKKβ, IκBα, p-IκB-α, nuclear p-p65 and total p65 were assessed using western blotting. (B) Bands were semi-quantitatively analyzed using ImageJ software, and normalized to β-actin or Histone H3 density. Data are presented as the mean ± SD of three independent experiments. *P<0.05, **P<0.01 vs. Control group; ##P<0.01 vs. HG + mimics NC group. HG, high glucose; miR, microRNA; NC, negative control; p-, phosphorylated.

miR-199a-3p inhibits HG-induced apoptosis and inflammatory response by targeting IKKβ. To investigate whether IKKβ was involved in the protective effects of miR-199a-3p against HG-induced inflammatory response and apoptosis, HK-2 cells were transfected with pcDNA-IKKβ plasmid together with miR-199a-3p mimics, followed by HG stimulation. IKKβ expression was markedly increased in HK-2 cells after

pcDNA-IKKβ transfection, as determined via western blotting (Fig. 6A). It was demonstrated that IKKβ overexpression attenuated the increased cell viability mediated by miR-199a-3p overexpression in HG treated HK-2 cells (Fig. 6B). It was also found that overexpression of IKKβ reversed the inhibition of cell apoptosis and activity of caspase-3 mediated by miR-199a-3p mimics in HG treated HK-2 (Fig. 6C-E). In
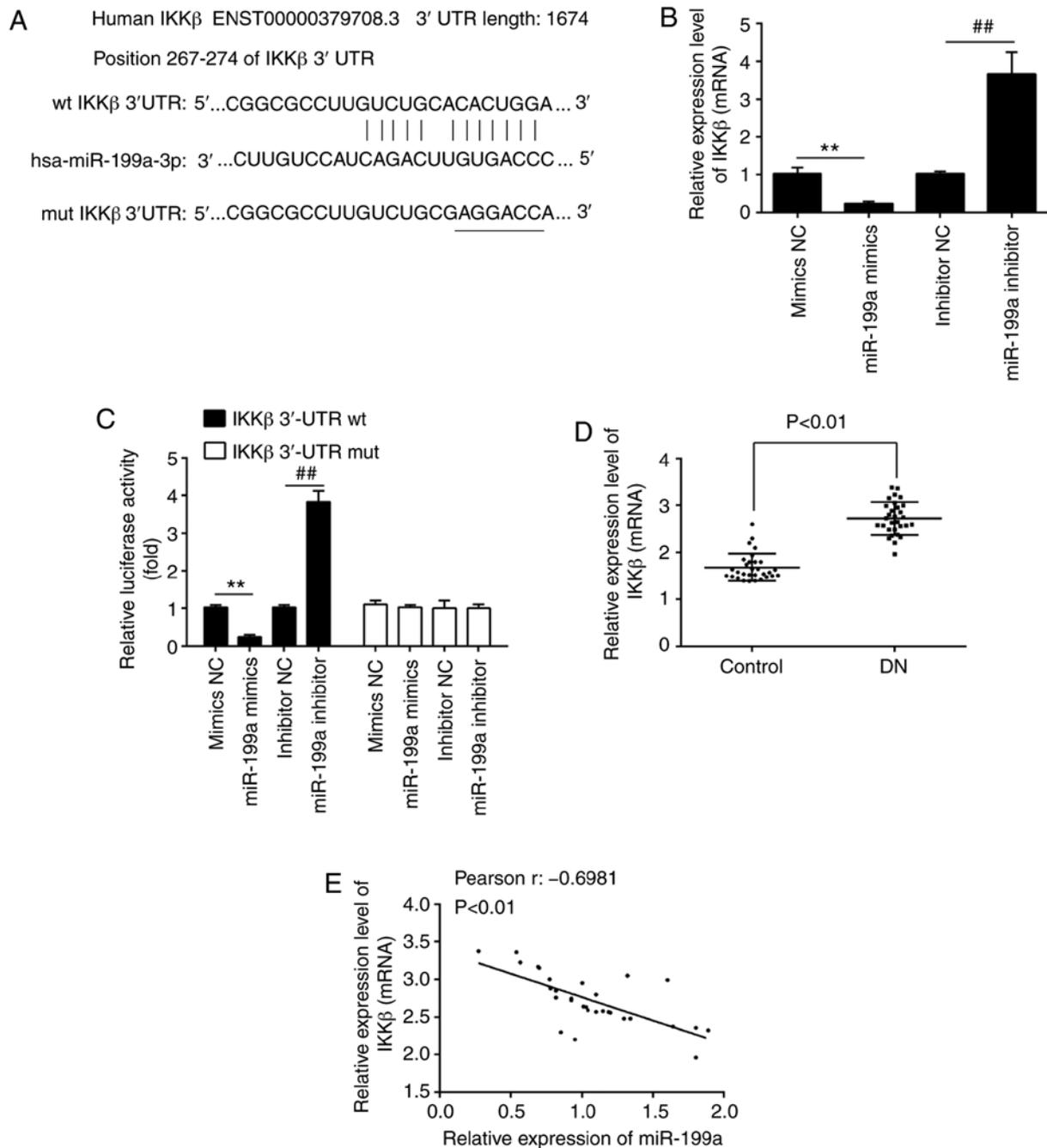
Figure 5. IKKβ is a direct target of miR-199a-3p in HK-2 cells. (A) Putative binding site of miR-199a-3p and IKKβ. (B) RT-qPCR analysis was used to assess the expression of IKKβ in HK-2 cells after miR-199a-3p mimics or miR-199a-3p inhibitor transfection. (C) HK-2 cells were co-transfected with firefly luciferase constructs containing the IKKβ wt or mut 3'UTRs and miR-199a-3p mimics, mimics NC, miR-199a-3p inhibitor or inhibitor NC. Then, the luciferase activity was analyzed using a dual-luciferase reporter assay system. Data are presented the mean ± SD of three independent experiments. **P<0.01 vs. mimics NC group; ##P<0.01 vs. inhibitor NC group. (D) RT-qPCR analysis was conducted to assess the expression of IKKβ in 30 peripheral blood samples from patients with DN and 30 peripheral blood samples from healthy controls. (E) Pearson's correlation was used to assess the correlation between miR-199a-3p and IKKβ expression levels in peripheral blood samples from patients with DN (r, -0.6981; P<0.01). RT-qPCR, reverse transcription-quantitative PCR; HG, high glucose; miR, microRNA; NC, negative control; wt, wild-type; mut, mutant; UTR, untranslated region.

addition, the increased expression of cleaved-caspase-3 caused by HG was attenuated by miR-199a-3p mimics, which was reversed by overexpression of IKKβ (Fig. 6F). The inhibitory effects of miR-199a-3p on HG-induced the releases of IL-8, IL-6 and TNF-α were also reversed by IKKβ overexpression (Fig. 6G-I). Collectively, these data suggested that miR-199a-3p exerted its anti-apoptotic and anti-inflammatory abilities by targeting IKKβ.

Discussion

In the present study, miR-199a-3p expression was downregulated in the peripheral blood samples of patients with DN, and was negatively correlated with the severity of DN. Moreover, it was observed that miR-199a-3p overexpression inhibited the apoptosis and inflammatory response by targeting the IKKβ/NF-κB pathway *in vitro*. These data suggested that
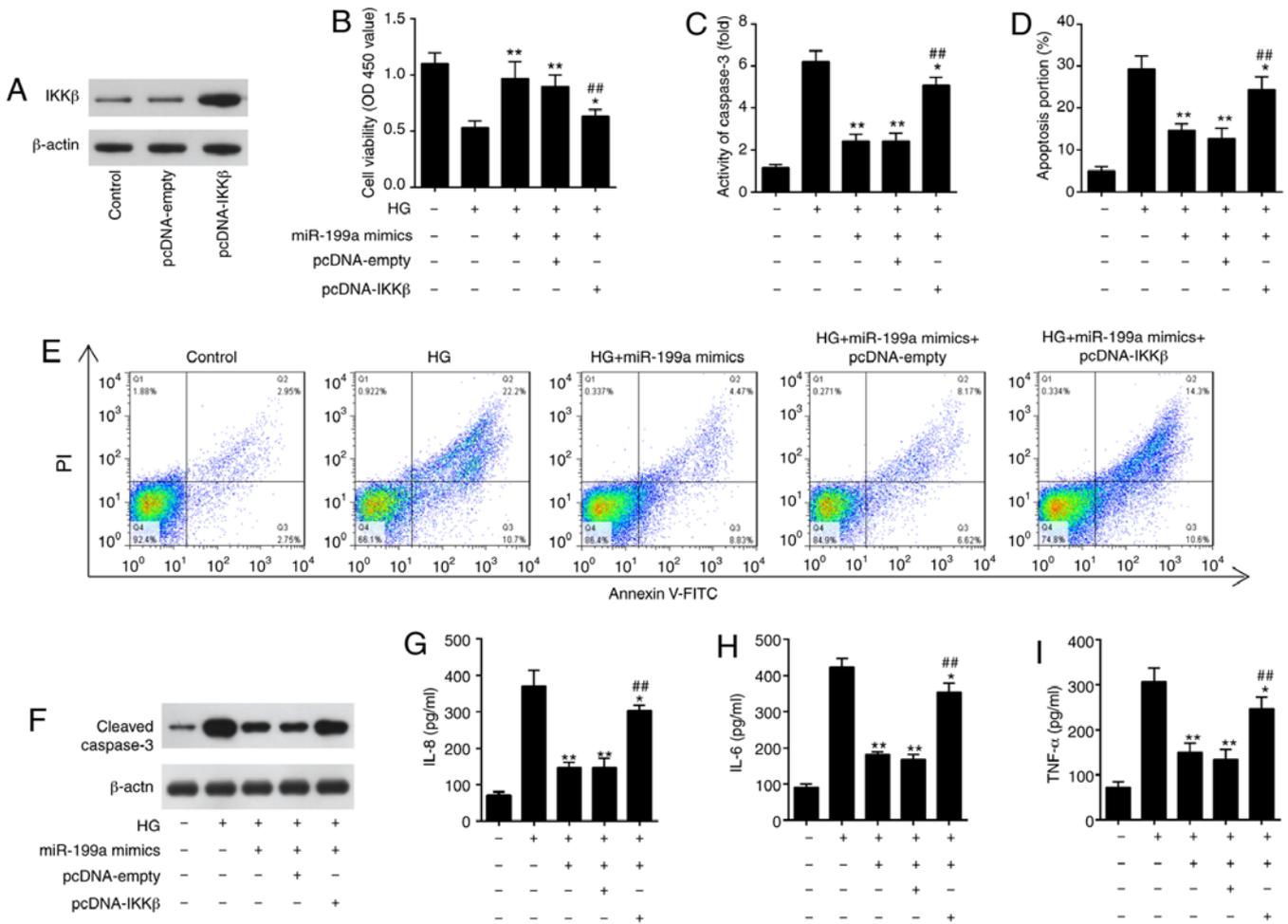
Figure 6. Overexpression of miR-199a-3p inhibits HG-induced HK-2 cell apoptosis and inflammation by targeting IKKβ. HK-2 cells were co-transfected with miR-199a-3p mimics and pcDNA-IKKβ for 24 h, followed by treatment with 30 mM HG for another 24 h, and then cells were harvested for subsequent experiments. (A) IKKβ protein expression in transfected HK-2 was analyzed via western blot analysis at 24 h post-transfection. (B) Cell viability was assessed using Cell Counting Kit-8 assay. (C) Activity of caspase-3 was measured using a caspase-3 Activity Assay kit. (D) Apoptosis was measured using (E) flow cytometry. (F) Cleaved-caspase-3 protein expression in transfected HK-2 was analyzed via western blotting. Levels of (G) IL-8, (H) IL-6 and (I) TNF-α were measured using ELISA kits. Data are presented as the mean ± SD of three independent experiments. *P<0.05, **P<0.01 vs. control group; ##P<0.01 vs. HG + miR-199a-3p mimics group. HG, high glucose; miR, microRNA; OD, optical density.

miR-199a-3p may act as a promising therapeutic target for DN.

Increasing evidence has revealed that miRNAs serve critical roles in the pathogenesis of DN. For example, Wang *et al* (26) reported that miR-424 overexpression prevented the occurrence and progression of DN by targeting RPTOR independent companion of MTOR complex 2 in rats. Moreover, Yang *et al* (27) observed that miR-214 suppressed oxidative stress in DN via the reactive oxygen species/Akt/mTOR signaling pathway in proximal tubular cells. Bai *et al* (28) also found that miR-130b attenuated renal tubulointerstitial fibrosis via the repression of Snail in HG-treated NRK-52E cells. These studies indicated that targeting miRNAs may be an effective approach for DN treatment. In the present study, using a miRNA microarray assay, miR-199a-3p expression was identified to be downregulated in the peripheral blood samples of patients with DN. Furthermore, its expression was negatively correlated with proteinuria in patients with DN. These findings suggested that miR-199a-3p may serve important role in the pathogenesis of DN.

miR-199a-3p has been observed to be frequently downregulated in several cancerous tissues and to influence various malignant processes, such as tumor growth, invasion and metastasis. For example, miR-199a-3p decreases esophageal cancer cell proliferation by targeting p21 activated kinase 4 (29). Liu *et al* (30) also found that overexpression of miR-199a-3p suppressed the cellular proliferation, colony formation, invasion and migration in clear cell renal cell carcinoma. However, other studies have reported increased expression of miR-199a-3p in various cancer types, including prostate cancer (31) and hepatocellular carcinoma (32), which contradicts the tumor suppressive role of this miRNA (33). In addition, several studies have demonstrated that miR-199a-3p has protective role in multiple types of cell injuries. For example, Dai *et al* (34) revealed that elevated miR-199-5p expression disrupted sustained endoplasmic reticulum stress and prevented hepatocytes from undergoing bile acid- or thapsigargin-induced cell death. Furthermore, Tao *et al* (35) found that miR-199a-3p promoted cardiomyocyte proliferation by inhibiting CD151 expression. Therefore, targeting miR-199a-3p

may be benefit for the treatment of human diseases, but the precise mechanisms vary in different cell types.

Previous studies have reported that miR-199a-3p exerts anti-inflammatory and anti-apoptotic effects in various diseases (36,37). For example, Liu *et al* (38) revealed that miR-199a-3p decreased pro-inflammatory cytokines expression levels in alveolar macrophages and septic lung tissues of mice. In addition, Wang *et al* (39) observed that evaluated miR-199a-3p attenuated TNF-α-induced apoptosis in human nucleus pulposus cells by targeting MAP3K5. It has also been demonstrated that miR-199a-3p overexpression improves cerebral ischemic injury via the inhibition of neuronal apoptosis and suppression of the inflammatory response in rats (40). Notably, miR-199a-3p has previously been reported to be downregulated in the urine of patients with DN (22). Additionally, it has been revealed that miR-199a-3p exerts anti-apoptotic and anti-inflammatory roles in various types of cells, such as human nucleus pulposus cells, kidney cells, hepatocytes, liver sinusoidal endothelial cells and retinal microglia cells (23-28). miR-199a-3p has been previously reported to be decreased in the urine from the patients with DN, which suggests that urine miR-199a-3p could be used as a potential biomarker for DN (41). However, to the best of our knowledge, the function of miR-199a-3p in the apoptosis and inflammatory response of RTEC in DN has not been previously reported. Thus, the present study aimed to investigate the effect of miR-199a-3p in DN. Using a HG-induced HK-2 cell injury model, the present study demonstrated that miR-199a-3p attenuated HG-induced the apoptosis and release of pro-inflammatory factors in HK-2 cells. These results suggested that miR-199a-3p exerted its protective role against HG-induced RTEC injury via the suppression of apoptosis and the inflammatory response.

The NF-κB pathway serves a pivotal role in HG-induced injury by regulating the inflammatory response (42-44). With regards to the pathological progression in DN, Kuhad and Chopra (45) reported that suppression of the NF-κB pathway using NF-κB inhibitors protected renal functions via the suppression of the inflammatory response in diabetic rats. Xie *et al* (46) have also shown that Carnosic acid improved DN by inhibiting the NF-κB pathway in streptozotocin-induced diabetic mice. Moreover, Ohga *et al* (47) demonstrated that thiazolidinedione (a PPAR-γ agonist) treatment ameliorated renal injury in experimental diabetic rats via anti-inflammatory effects mediated by inhibiting NF-κB activation. In addition to being an inflammatory regulator, the NF-κB pathway also controls the expression levels of key genes involved in apoptosis, such as Bax and Bcl-2 (48,49). For example, it has been reported that suppression of the NF-κB pathway contributes to a decrease in apoptosis induced by HG in HK-2 cells (50). The present findings suggested that miR-199a-3p overexpression suppressed HG-induced activation of the NF-κB pathway in HK-2 cells, indicating that miR-199a-3p exerted its anti-apoptotic and anti-inflammation activities via the regulation of the NF-κB pathway. However, the mechanism of miR-199a-3p-mediated regulation of NF-κB is yet to be fully elucidated.

The NF-κB signaling pathway is one of the most important pathways mediating the generation of inflammatory factors, including TNF-α, IL-6 and IL-8, in various types of cells, such as bronchial epithelial cells, periodontal ligament cells, endothelial cells and colorectal cancer cells (51-54). In the present study, decreased TNF-α, IL-6 and IL-8 expression levels were observed after miR-199a-3p transfection, and were accompanied with reduced NF-κB activation. These results suggested that miR-199a-3p may function, at least in part, via the NF-κB pathway to downregulate the expression levels of inflammatory factors.

IKKβ, one of the catalytic subunits of the IKK complex, is the major kinase controlling the canonical pathway of NF-κB activation, in which phosphorylation of IκB by IKK releases NF-κB to enter nucleus, where it binds to cognate sequences in the promoter region of multiple genes (55). It has been reported that IKKβ acts as a downstream molecule of certain miRNAs to mediate the role of the miRNAs in various cell types, including miR-199a (56). For example, miR-199a-3p suppresses IKKβ to inhibit NF-κB activity, which reduces the malignancy of oral squamous cell carcinoma cells (57). Dai *et al* (58) also revealed that miR-199a attenuated the invasive capability of endometrial stromal cells via the suppression of IKKβ, which inhibited the activation of the NF-κB pathway. Moreover, Chen *et al* (59) reported that miR-199a could affect NF-κB activity in ovarian cancer cells by targeting IKKβ. Previous studies have also shown that miR-199a inhibits the activation of the NF-κB signaling pathway in cancer cells and renal cells (59,60). Therefore, it was suggested that miR-199a-3p regulates the NF-κB pathway in DN. In the current study, IKKβ was identified to be targeted by miR-199a-3p. Further experimental results indicated that IKKβ expression in HK-2 cells was upregulated, and was negatively correlated with miR-199a-3p in patients with DN. It was demonstrated that IKKβ overexpression alleviated the inhibitory effects of miR-199a-3p overexpression on inflammation and apoptosis in HG-treated HK-2 cells. Collectively, the present findings indicated that miR-199a-3p exerted its anti-inflammatory and anti-apoptotic effects via the IKKβ/NF-κB pathway in HG-treated HK-2 cells.

However, there are limitations to the present study. DN is a complex pathological process involving numerous miRNAs and target genes. The main limitation of this study is the sole focus on the IKKβ/NF-κB pathway. The underlying relationship between this pathway and other related pathways requires further investigations.

In conclusion, the current findings demonstrated that the miR-199a-3p was downregulated in patients with DN, and miR-199a-3p overexpression improved HG-induced inflammation and apoptosis by blocking the IKKβ/NF-κB pathway. These findings support the hypothesis that enhanced miR-199a-3p expression may serve as a novel therapeutic approach for the treatment of DN.

Availability of data and materials

The miRNA microarray datasets generated and/or analyzed during the current study are not publicly available due to other

research on the microarray that is under way, but are available from the corresponding author on reasonable request. Other data generated or analyzed during the present study are included in this published article.

Authors' contributions

Conceived and designed the experiments: JS. Performed the experiments: RZ and LQ. Analyzed the data: RZ and LQ. Contributed reagents, materials and analysis tools: JS. Wrote the paper: RZ and JS. All authors have read and approved the final version of manuscript.

Ethics approval and consent to participate

All individuals provided informed consent for the use of human specimens for clinical research. The present study was approved by the Huaihe Hospital of Henan University Ethics Committees.

Patient consent for publication

Not applicable.

Competing interests

The authors declare that they have no competing interests.

References

1. Umanath K and Lewis JB: Update on diabetic nephropathy: Core curriculum 2018. Am J Kidney Dis 71: 884-895, 2018.
2. Verzola D, Gandolfo MT, Ferrario F, Rastaldi MP, Villaggio B, Gianiorio F, Giannoni M, Rimoldi L, Lauria F, Miji M, *et al*: Apoptosis in the kidneys of patients with type II diabetic nephropathy. Kidney Int 72: 1262-1272, 2007.
3. Magri CJ and Fava S: The role of tubular injury in diabetic nephropathy. Eur J Intern Med 20: 551-555, 2009.
4. Li T and Cho WC: MicroRNAs: Mechanisms, functions and progress. Genomics Proteomics Bioinformatics 10: 237-238, 2012.
5. Zhu FX, Wu HL, Chen JX, Han B and Guo YF: Dysregulation of microRNA-181b and TIMP3 is functionally involved in the pathogenesis of diabetic nephropathy. J Cell Physiol 234: 18963-18969, 2019.
6. Bhatt K, Lanting LL, Jia Y, Yadav S, Reddy MA, Magilnick N, Boldin M and Natarajan R: Anti-inflammatory role of MicroRNA-146a in the pathogenesis of diabetic nephropathy. J Am Soc Nephrol 27: 2277-2288, 2016.
7. Deshpande SD, Putta S, Wang M, Lai JY, Bitzer M, Nelson RG, Lanting LL, Kato M and Natarajan R: Transforming growth factor-β-induced cross talk between p53 and a microRNA in the pathogenesis of diabetic nephropathy. Diabetes 62: 3151-3162, 2013.
8. Long J, Wang Y, Wang W, Chang BH and Danesh FR: Identification of microRNA-93 as a novel regulator of vascular endothelial growth factor in hyperglycemic conditions. J Biol Chem 285: 23457-23465, 2010.
9. Wang J, Gao Y, Ma M, Li M, Zou D, Yang J, Zhu Z and Zhao X: Effect of miR-21 on renal fibrosis by regulating MMP-9 and TIMP1 in kk-ay diabetic nephropathy mice. Cell Biochem Biophys 67: 537-546, 2013.
10. Li H, Zhu X, Zhang J and Shi J: MicroRNA-25 inhibits high glucose-induced apoptosis in renal tubular epithelial cells via PTEN/AKT pathway. Biomed Pharmacother 96: 471-479, 2017.
11. Li X, Zeng L, Cao C, Lu C, Lian W, Han J, Zhang X, Zhang J, Tang T and Li M: Long noncoding RNA MALAT1 regulates renal tubular epithelial pyroptosis by modulated miR-23c targeting of ELAVL1 in diabetic nephropathy. Exp Cell Res 350: 327-335, 2017.
12. Lau GJ, Godin N, Maachi H, Lo CS, Wu SJ, Zhu JX, Brezniceanu ML, Chénier I, Fragasso-Marquis J, Lattouf JB, *et al*: Bcl-2-modifying factor induces renal proximal tubular cell apoptosis in diabetic mice. Diabetes 61: 474-484, 2012.
13. Huang YF, Zhang Y, Liu CX, Huang J and Ding GH: microRNA-125b contributes to high glucose-induced reactive oxygen species generation and apoptosis in HK-2 renal tubular epithelial cells by targeting angiotensin-converting enzyme 2. Eur Rev Med Pharmacol Sci 20: 4055-4062, 2016.
14. Su J, Ren J, Chen H and Liu B: MicroRNA-140-5p ameliorates the high glucose-induced apoptosis and inflammation through suppressing TLR4/NF-κB signaling pathway in human renal tubular epithelial cells. Biosci Rep 40: BSR20192384, 2020.
15. Lv L, Zhang J, Tian F, Li X, Li D and Yu X: Arbutin protects HK-2 cells against high glucose-induced apoptosis and autophagy by up-regulating microRNA-27a. Artif Cells Nanomed Biotechnol 47: 2940-2947, 2019.
16. Wang GJ, Jiao BP, Liu YJ, Li YR and Deng BB: Reactivation of microRNA-506 inhibits gastric carcinoma cell metastasis through ZEB2. Aging (Albany NY) 11: 1821-1831, 2019.
17. Kohl M, Wiese S and Warscheid B: Cytoscape: Software for visualization and analysis of biological networks. Methods Mol Biol 696: 291-303, 2011.
18. Livak KJ and Schmittgen TD: Analysis of relative gene expression data using real-time quantitative PCR and the 2(-Delta Delta C(T)) method. Methods 25: 402-408, 2001.
19. Ding Y, Wang L, Zhao Q, Wu Z and Kong L: MicroRNA93 inhibits chondrocyte apoptosis and inflammation in osteoarthritis by targeting the TLR4/NFkB signaling pathway. Int J Mol Med 43: 779-790, 2019.
20. Wang X, Shen E, Wang Y, Li J, Cheng D, Chen Y, Gui D and Wang N: Cross talk between miR-214 and PTEN attenuates glomerular hypertrophy under diabetic conditions. Sci Rep 6: 31506, 2016.
21. Zha F, Bai L, Tang B, Li J, Wang Y, Zheng PX, Ji T and Bai S: MicroRNA-503 contributes to podocyte injury via targeting E2F3 in diabetic nephropathy. J Cell Biochem 120: 12574-12581, 2019.
22. Chen YY, Peng XF, Liu GY, Liu JS, Sun L, Liu H, Xiao L and He LY: Protein arginine methyltranferase-1 induces ER stress and epithelial-mesenchymal transition in renal tubular epithelial cells and contributes to diabetic nephropathy. Biochim Biophys Acta Mol Basis Dis 1865: 2563-2575, 2019.
23. Ni WJ, Tang LQ and Wei W: Research progress in signalling pathway in diabetic nephropathy. Diabetes Metab Res Rev 31: 221-233, 2015.
24. Yu C, Qi D, Sun JF, Li P and Fan HY: Rhein prevents endotoxin-induced acute kidney injury by inhibiting NF-κB activities. Sci Rep 5: 11822, 2015.
25. Yang X, Wang Y and Gao G: High glucose induces rat mesangial cells proliferation and MCP-1 expression via ROS-mediated activation of NF-κB pathway, which is inhibited by eleutheroside E. J Recept Signal Transduct Res 36: 152-157, 2016.
26. Wang G, Yan Y, Xu N, Hui Y and Yin D: Upregulation of microRNA-424 relieved diabetic nephropathy by targeting rictor through mTOR complex2/protein kinase B signaling. J Cell Physiol 234: 11646-11653, 2019.
27. Yang S, Fei X, Lu Y, Xu B, Ma Y and Wan H: miRNA-214 suppresses oxidative stress in diabetic nephropathy via the ROS/Akt/mTOR signaling pathway and uncoupling protein 2. Exp Ther Med 17: 3530-3538, 2019.
28. Bai X, Geng J, Zhou Z, Tian J and Li X: MicroRNA-130b improves renal tubulointerstitial fibrosis via repression of Snail-induced epithelial-mesenchymal transition in diabetic nephropathy. Sci Rep 6: 20475, 2016.
29. Phatak P, Burrows WM, Chesnick IE, Tulapurkar ME, Rao JN, Turner DJ, Hamburger AW, Wang JY and Donahue JM: MiR-199a-3p decreases esophageal cancer cell proliferation by targeting p21 activated kinase 4. Oncotarget 9: 28391-28407, 2018.
30. Liu J, Liu B, Guo Y, Chen Z, Sun W, Gao W, Wu H and Wang Y: MiR-199a-3p acts as a tumor suppressor in clear cell renal cell carcinoma. Pathol Res Pract 214: 806-813, 2018.
31. Qu F, Zheng J, Gan W, Lian H, He H, Li W, Yuan T, Yang Y, Li X, Ji C, *et al*: MiR-199a-3p suppresses proliferation and invasion of prostate cancer cells by targeting Smad1. Oncotarget 8: 52465-52473, 2017.
32. Callegari E, D'Abundo L, Guerriero P, Simioni C, Elamin BK, Russo M, Cani A, Bassi C, Zagatti B, Giacomelli L, *et al*: miR-199a-3p modulates MTOR and PAK4 pathways and inhibits tumor growth in a hepatocellular carcinoma transgenic mouse model. Mol Ther Nucleic Acids 11: 485-493, 2018.

33. Li L, Mou YP, Wang YY, Wang HJ and Mou XZ: miR-199a-3p targets ETNK1 to promote invasion and migration in gastric cancer cells and is associated with poor prognosis. Pathol Res Pract 215: 152511, 2019.
34. Dai BH, Geng L, Wang Y, Sui CJ, Xie F, Shen RX, Shen WF and Yang JM: microRNA-199a-5p protects hepatocytes from bile acid-induced sustained endoplasmic reticulum stress. Cell Death Dis 4: e604, 2013.
35. Tao Y, Zhang H, Huang S, Pei L, Feng M, Zhao X, Ouyang Z, Yao S, Jiang R and Wei K: miR-199a-3p promotes cardiomyocyte proliferation by inhibiting Cd151 expression. Biochem Biophys Res Commun 516: 28-36, 2019.
36. Rane S, He M, Sayed D, Vashistha H, Malhotra A, Sadoshima J, Vatner DE, Vatner SF and Abdellatif M: Downregulation of miR-199a derepresses hypoxia-inducible factor-1alpha and Sirtuin 1 and recapitulates hypoxia preconditioning in cardiac myocytes. Circ Res 104: 879-886, 2009.
37. Zuo Y, Wang Y, Hu H and Cui W: Atorvastatin protects myocardium against ischemia-reperfusion injury through inhibiting miR-199a-5p. Cell Physiol Biochem 39: 1021-1030, 2016.
38. Liu Y, Guan H, Zhang JL, Zheng Z, Wang HT, Tao K, Han SC, Su LL and Hu D: Acute downregulation of miR-199a attenuates sepsis-induced acute lung injury by targeting SIRT1. Am J Physiol Cell Physiol 314: C449-C455, 2018.
39. Wang W, Guo Z, Yang S, Wang H and Ding W: Upregulation of miR-199 attenuates TNF-α-induced human nucleus pulposus cell apoptosis by downregulating MAP3K5. Biochem Biophys Res Commun 505: 917-924, 2018.
40. Li M, Luan L, Liu Q, Liu Y, Lan X, Li Z and Liu W: MiRNA-199a-5p protects against cerebral ischemic injury by down-regulating DDR1 in rats. World Neurosurg 131: e486-e494, 2019.
41. Meng L, Li G, Liu X, Jiang J, Zhu M and Sun Y: Decreased urine miR-199-3p may be a potential biomarker for diabetic nephropathy via targeting zinc finger e-box-bindingprotein 1. Clin Lab 64: 1177-1182, 2018.
42. Gu J, Huang W, Zhang W, Zhao T, Gao C, Gan W, Rao M, Chen Q, Guo M, Xu Y and Xu YH: Sodium butyrate alleviates high-glucose-induced renal glomerular endothelial cells damage via inhibiting pyroptosis. Int Immunopharmacol 75: 105832, 2019.
43. Kang Z, Zeng J, Zhang T, Lin S, Gao J, Jiang C, Fan R and Yin D: Hyperglycemia induces NF-κB activation and MCP-1 expression via downregulating GLP-1R expression in rat mesangial cells: Inhibition by metformin. Cell Biol Int 43: 940-953, 2019.
44. Li J, Tang Y and Cai D: IKKβ/NF-κB disrupts adult hypothalamic neural stem cells to mediate a neurodegenerative mechanism of dietary obesity and pre-diabetes. Nat Cell Biol 14: 999-1012, 2012.
45. Kuhad A and Chopra K: Attenuation of diabetic nephropathy by tocotrienol: Involvement of NFkB signaling pathway. Life Sci 84: 296-301, 2009.
46. Xie Z, Zhong L, Wu Y, Wan X, Yang H, Xu X and Li P: Carnosic acid improves diabetic nephropathy by activating Nrf2/ARE and inhibition of NF-κB pathway. Phytomedicine 47: 161-173, 2018.
47. Ohga S, Shikata K, Yozai K, Okada S, Ogawa D, Usui H, Wada J, Shikata Y and Makino H: Thiazolidinedione ameliorates renal injury in experimental diabetic rats through anti-inflammatory effects mediated by inhibition of NF-kappaB activation. Am J Physiol Renal Physiol 292: F1141-F1150, 2007.
48. Leibowitz B and Yu J: Mitochondrial signaling in cell death via the Bcl-2 family. Cancer Biol Ther 9: 417-422, 2010.
49. Nam MS, Jung DB, Seo KH, Kim BI, Kim JH, Kim JH, Kim B, Baek NI and Kim SH: Apoptotic effect of sanggenol L via caspase activation and inhibition of NF-κB signaling in ovarian cancer cells. Phytother Res 30: 90-96, 2016.
50. Lu J, Peng J, Xiang M, He L, Wang D, Xiong G and Li S: Trichosanthes kirilowii lectin alleviates diabetic nephropathy by inhibiting the LOX1/NF-κB/caspase-9 signaling pathway. Biosci Rep 38: BSR20180071, 2018.
51. Abolhassani M, Aloulou N, Chaumette MT, Aparicio T, Martin-Garcia N, Mansour H, Gouvello SL, Delchier JC and Sobhani I: Leptin receptor-related immune response in colorectal tumors: The role of colonocytes and interleukin-8. Cancer Res 68: 9423-9432, 2008.
52. Fang Y, Shi C, Manduchi E, Civelek M and Davies PF: MicroRNA-10a regulation of proinflammatory phenotype in athero-susceptible endothelium in vivo and in vitro. Proc Natl Acad Sci USA 107: 13450-13455, 2010.
53. Kanoh S, Tanabe T and Rubin BK: Dapsone inhibits IL-8 secretion from human bronchial epithelial cells stimulated with lipopolysaccharide and resolves airway inflammation in the ferret. Chest 140: 980-990, 2011.
54. Chi XP, Ouyang XY and Wang YX: Hydrogen sulfide synergistically upregulates porphyromonas gingivalis lipopolysaccharide-induced expression of IL-6 and IL-8 via NF-κB signalling in periodontal fibroblasts. Arch Oral Biol 59: 954-961, 2014.
55. Caamaño J and Hunter CA: NF-kappaB family of transcription factors: Central regulators of innate and adaptive immune functions. Clin Microbiol Rev 15: 414-429, 2002.
56. Bardin P, Marchal-Duval E, Sonneville F, Blouquit-Laye S, Rousselet N, Rouzic PL, Corvol H and Tabary O: Small RNA and transcriptome sequencing reveal the role of miR-199a-3p in inflammatory processes in cystic fibrosis airways. J Pathol 245: 410-420, 2018.
57. Wei D, Shen B, Wang W, Zhou Y, Yang X, Lu G, Yang J and Shao Y: MicroRNA199a5p functions as a tumor suppressor in oral squamous cell carcinoma via targeting the IKKβ/NFkB signaling pathway. Int J Mol Med 43: 1585-1596, 2019.
58. Dai L, Gu L and Di W: MiR-199a attenuates endometrial stromal cell invasiveness through suppression of the IKKβ/NF-κB pathway and reduced interleukin-8 expression. Mol Hum Reprod 18: 136-145, 2012.
59. Chen R, Alvero AB, Silasi DA, Kelly MG, Fest S, Visintin I, Leiser A, Schwartz PE, Rutherford T and Mor G: Regulation of IKKbeta by miR-199a affects NF-kappaB activity in ovarian cancer cells. Oncogene 27: 4712-4723, 2008.
60. Wu C, Lv C, Chen F, Ma X, Shao Y and Wang Q: The function of miR-199a-5p/Klotho regulating TLR4/NF-κB p65/NGAL pathways in rat mesangial cells cultured with high glucose and the mechanism. Mol Cell Endocrinol 417: 84-93, 2015.